The role and mechanism of exosomes from umbilical cord mesenchymal stem cells in inducing osteogenesis and preventing osteoporosis

Yahao Ge
Second Affiliated Hospital of Shantou University Medical College https://orcid.org/0000-0001-9691-5376

Xinjia Wang (xj.wang2000@163.com)
https://orcid.org/0000-0002-5756-5382

Research

Keywords: Umbilical cord mesenchymal stem cells, Exosomes, Microenvironment, Osteoporosis, MicroRNA, Osteogenic differentiation

DOI: https://doi.org/10.21203/rs.3.rs-37420/v1

Abstract

Background

Mesenchymal stem cell (MSC) exosomes promote tissue regeneration and repair, and thus might be used to treat many diseases; however, the influence of microenvironmental conditions on exosomes remains unclear. The present study aimed to analyze the effect of the osteogenic differentiation microenvironment on the functions of human umbilical cord MSCs (HucMSC)-derived exosomes. We explored the role and mechanism by which exosomes promote osteogenic differentiation and prevent osteoporosis, and propose a method to treat and prevent osteoporosis.

Methods

HucMSCs were isolated from human umbilical cords, and after osteogenic differentiation and normal culture for 48 h, cell supernatants were collected to isolate exosomes. Exosomes from standardized stem cell culture (Exo1) and osteogenic differentiation-exosomes (Exo2) were co-cultured with osteoblasts, separately. Cell counting kit-8 assays, and alkaline phosphatase and alizarin red staining were used to observe the exosomes' effects on osteoblast proliferation and differentiation. The levels of osteogenic differentiation-related proteins were analyzed using western blotting. Estrogen-deficient osteoporosis model mice were established, and treated with the two exosomes preparations. Micro-computed tomography and hematoxylin and eosin staining were performed after 6 weeks. MicroRNAs in Exo1 and Exo2 were sequenced and analyzed using bioinformatics.

Results

Treatment with Exo1 and Exo2 enhanced osteoblast osteogenic differentiation significantly, and osteogenic differentiation-related gene and protein expression increased significantly in a concentration-dependent manner. Compared with Exo1 group, Exo2 had a stronger osteogenic differentiation promoting effect, but a weaker proliferation promoting effect. Exo1 and Exo2 significantly improved the tibial density of osteoporosis model mice, with no significant differences between the groups. Sequencing and bioinformatics analysis showed that hsa-mir-328-3p and hsa-mir-2110 might be exosome osteogenesis regulatory microRNAs. Compared with Exo1, the target genes of Exo2-carried microRNAs are enriched in osteoclast differentiation and PPAR signaling.

Conclusions

HucMSC-derived exosomes can promote osteogenic differentiation. Exosomes produced in an osteogenic differentiation microenvironment had a stronger osteogenic function, but a weaker proliferative effect. HucMSC-derived exosomes have a therapeutic effect on osteoporosis. The exosomes induced by osteoblasts carry microRNAs that regulate osteoblast differentiation, which might function via osteoblast, adipocyte, and osteoclast differentiation signaling pathways.

Background

Mesenchymal stem cells (MSCs) have the potential for multidirectional differentiation, immune regulation, and tissue repair and regeneration, and have therapeutic effects on a variety of orthopedic diseases [1]. However, studies have found that after MSC transplantation, the number of cells remains very small, and the substitution effect of local cell differentiation is insufficient to support complex pathological changes [1, 2], suggesting that local proliferation and differentiation of MSCs might not be the mechanism by which MSCs exert their therapeutic effects. Recent studies have found that exosomes play an important role in intercellular communication [3,4]. MSC-derived exosomes contain a variety of bioactive substances, and have the functions of low immunogenicity, immune regulation, promoting proliferation, and promoting tissue repair. For example, MSC-derived exosomes have therapeutic effects on diabetes, renal disease, and ischemic stroke [5,6]. MicroRNAs (miRNAs) are one of the main bioactive substances in exosomes, and comprise endogenous non-coding single-stranded small RNAs (18–25 nucleotides in length) that regulate gene expression at the post-transcriptional level by binding to the 3' untranslated region (UTR) region of target mRNAs [7]. Experimental studies have confirmed that miRNAs in MSC-derived exosomes play an important role in regulating cell function and treating various diseases [8]. For example, by targeting *WNT5A* (Wnt family member 5A), high expression of exosome-derived miR-92a-3p in MSCs could promote cartilage regeneration [9]. However, the secretion and function of exosomes are greatly influenced by the cell state and microenvironment. For example, in the microenvironment of tumor formation, MSC-derived exosomes promote the disappearance of normal functions of tissue repair, and changes to the exosome cargoes can promote the proliferation and invasion of tumor cells, and lead to the transformation of normal stromal cells to tumor fibroblasts [10].

Human umbilical cord MSCs (HucMSCs) can be collected in a non-invasive manner, and have a strong regenerative ability [11], resulting in them having broad application prospects in regenerative medicine. However, the effect of the osteogenic differentiation microenvironment on the function of exosomes remains unclear. In the present study, we aimed to analyze the effects of exosomes secreted by HucMSCs in the microenvironment of osteogenic differentiation on the proliferation and differentiation of osteoblasts, and to explore the changes of exosome function in the microenvironment. The exosomes were applied to treat an osteoporosis animal model. High-throughput gene sequencing and bioinformatics techniques were used to analyze the differential expression of exosomal miRNAs, to reveal the relevant molecular mechanisms of exosome action, and provide new targets to treat and prevent osteoporosis.

Methods

Isolation and characterization of hucMSCs

Umbilical cords were obtained from healthy newborn fetuses, and Wharton's jelly tissues were isolated under sterile conditions. Tissues were cut to 1–2 mm^3 size tissue pieces and inoculated in culture flasks containing 10% fetal bovine serum (FBS) in a cell incubator at 37 °C and 5% CO_2 saturated humidity.

When cells grew to 80% confluence, tissue blocks were removed, digested, and subcultured with 0.25% trypsin (Gibco, Grand Island, NY, USA) containing EDTA. HucMSCs of Passage 3 were taken and the cell concentration was adjusted to 1 ´ 10^6/ml. Antibodies labeled with fluorescein isothiocyanate (FITC), Peridinin chlorophyll protein complex (PerCP)-cyanine (Cy)ä5.5, Allophycocyanin (APC), and Phycoerythrin (PE) were used (FITC-CD90, PerCP-Cyä5.5-CD105, APC-CD73, PE-CD45, PE-CD34, PECD11b, PE-CD19, and PE-HLA-DR) (BD Stemflow hMSC Analysis Kit). The cells were incubated with the antibodies at room temperature for 30 min, washed with phosphate-buffered saline (PBS), centrifuged at 300×g for 5 min, and the supernatant discarded. The cells were resuspended in PBS and analyzed using flow cytometry (BD Biosciences, San Jose, CA, USA). HucMSCs of Passage 3 were seeded in 24-well cell culture plates (Corning, NY, USA). When the cells grew to 80–90% confluence, they were replaced with osteogenic differentiation induction conditioned medium, adipose differentiation conditioned medium, or cartilage differentiation conditioned medium (Cyagen Biosciences, Guangzhou, China). After 21 days of induced differentiation, osteogenic differentiation was detected using with Alizarin red staining, and adipose differentiation was detected using oil red staining.

Isolation and characterization of exosomes derived from HucMSCs

HucMSC-Exosome (Exo1): HucMSCs of passage 3 (P3) were cultured with Dulbecco's modified Eagle's medium (DMEM)/F12 conditioned medium containing 10% exosome-free FBS (System Biosciences, Palo Alto, CA, USA), and the cell supernatant was collected after 48 h of culture. Osteogenic differentiation-Exosome (Exo2): HucMSCs of P3 were cultured to 80% confluence, washed twice with PBS, and replaced with osteogenic induction differentiation conditioned medium containing 10% exosome-free FBS, with 50 M vitamin C, 10 mM beta-phosphoglycerol, and 0.1 M dexamethasone (Sigma, St. louis, MO, USA). Cell supernatants were collected after 48 h of culture.

Collected cell supernatants were subjected to 2000 ´ *g* gradient centrifugation (Eppendorf, Hamburg, Germany) at 4 °C for 20 min and the pellet was discarded. The supernatant was removed to a new centrifuge tube and centrifuged at 10,000 ´ *g* at 4 °C for 40 min. The pellet was discarded and the supernatant was removed to a new centrifuge tube. The pellet was collected by centrifugation at 100,000´ *g* for 60 min, resuspended by PBS and centrifuged at 100,000 ´ *g* (Beckman, USA) for 60 min at 4 °C. The pellets were resuspended in PBS, and then filtered and sterilized through 0.22 μm sterile filter membrane, and stored in a freezer (Panasonic, Osaka, Japan) at -80 °C

After adjusting the exosome suspension to the appropriate concentration with PBS, the exosomes were dripped on special carbon-film copper mesh for electron microscopy observation. The exosomes on the mesh were stained with 2% phosphotungstic acid for 2–3 min, air-dried naturally, and photographed using transmission electron microscopy (Hitachi, Tokyo, Japan). Western blotting was used to detect three exosome-derived proteins, CD9, CD81, and HSP70 (ProteinTech, Rosemont, IL, USA). Vesicle diameter in the exosome suspensions was measured using particle size analyzer (Malvern Nanosight NS300, Malvern, UK).

Isolation of osteoblasts

Osteoblasts (OBs) were derived from the skulls of suckling SD rats. OBs in the skull were isolated using an appropriate amount of 0.2% type II collagenase (Gibco□NY□USA) and inoculated into T75 culture flasks (Corning, NY, USA) containing DMEM medium (Gibco□NY□USA) (containing 10% FBS, penicillin 100 U/ml, streptomycin 0.1 mg/ml).

Cell Counting Kit-8 (CCK-8)

The isolated OBs were seeded into 96-well plates at a concentration of 3 ´ 10^3/ml, and 100 μL of cell suspension was added into each well. After 12 h, Exo1 and Exo2 were co-cultured with the OBs at three concentration of 0, 0.05, 0.1, and 0.2 mg/ml. Four control duplicate wells were set at each concentration. After incubation for 36 and 60 h, 10 μl of CCK-8 (MCE, Monmouth Junction, NJ, USA) reagent was added to each well, and after incubation at 37 °C for 2 h in the dark, the absorbance at 450 nm wavelength was detected using a microplate reader (Tecan, Männedorf, Switzerland).

Alkaline phosphatase (ALP) and alizarin red staining

The isolated OBs were seeded in 24-well plates, and after 24–48 h, when the cells had grown to 80% confluence, osteogenic induction was performed using osteogenic induction medium. Co-cultures with Exo1 and Exo2, at 0.2, 0.1, and 0 mg/ml were set, respectively. Each concentration gradient had four duplex holes, and the solution was changed every 3 days. Alkaline phosphatase kit(Beyotime, Shanghai, China) was used for analysis after 10 days. After 21 days, alizarin red (Solarbio, Beijing, China) staining was performed according to the manufacturer's instructions. The results for the groups were compared and analyzed according to the depth of staining.

Western Blotting

OBs were co-cultured with Exo1 and Exo2 in osteogenic induction medium conditions, respectively. Three concentration of 0.1, 0.2, and 0 mg/ml were set. After 7 days of culture, the cells were collected and 150 μL of Radioimmunoprecipitation assay (RIPA) Lysis Buffer (Beyotime, Shanghai, China) was added to each well of the 6-well plate for lysis. All protein concentrations were determined using a bicinchoninic acid (BCA) protein concentration determination kit (Beyotime). The protein concentrations in the samples were adjusted so that the protein content was the same in the same volume. The SDS-PAGE gel preparation kit (Beyotime) was used for constant voltage protein electrophoresis at 80 V for 40 min, followed by 120 V for 30 min. The separated proteins were transferred to PVDF membranes (0.2 μm; Thermo Scientific, Rockford, IL. USA) at 300 mA for 80 min. The membranes were the incubated in 10% skimmed milk (BD) for 1 h at room temperature, incubated overnight with primary antibodies at 4 °C, followed by incubation with horseradish peroxidase-labeled secondary antibody (Beyotime) at room temperature for 1 h. Immunoreactive proteins on the membranes were visualized using a chemiluminescent imager (Bio-Rad, Hercules, CA, USA) using extremely hypersensitive ECL luminescent reagents. The mouse-derived primary antibodies recognized target proteins of osteogenic differentiation

including RUNX family transcription factor 2 (RUNX2), osteopontin (OST), collagen type I alpha 1 Chain (COL1A1), and ALP (Abcam, Cambridge, MA, USA), and the internal reference was detected using mouse-derived anti-glyceraldehyde-3-phosphate dehydrogenase (GAPDH) antibodies (ProteinTech). The protein expression intensity was compared and analyzed according to the ratio of the gray value of target protein to the gray value of the internal reference protein.

Animal model of osteoporosis

This experimental study was approved by the Medical Laboratory Animal Ethics Committee, and all experimental procedures were in accordance with the procedures of the Medical Laboratory Animal Center of Shantou University Medical College. All C57BL/6J mice were purchased from Beijing Weitong Lihua Laboratory Animal Technology Co., Ltd (Beijing, China). Forty 10-week-old C57 female mice were divided into five groups with eight mice in each group: Sham group, ovariectomized (OVX) group, OVX+Exo1 group, OVX+Exo2 group, and OVX+E2 (estradiol) group. Referring to experimental studies such as Zhen Lian [12], all mice in the experimental group were anesthetized with 2% pentobarbital sodium. Except for the sham group, ovariectomy was performed to simulate the osteoporotic disease model caused by estrogen deficiency. The sham group underwent a sham operation as the control group. A small incision was made on the back of mice to remove the ovaries, including part of the fallopian tube, and the incision was sutured with 5-0 artificial absorbable sutures. After 1 week of recovery time, the experiment was carried out. The OVX+Exo1 group, OVX+Exo2 group, and OVX+E2 group were intraperitoneally injected with Exo1 (0.5 mg/kg), Exo2 (0.5 mg/kg), and E2 (0.15 mg/kg), respectively. The OVX group was injected with the same volume of PBS. Injection every 3 days for 6 weeks.

Six weeks later, the tibia of mice were taken, and five groups were subjected to micro computed tomography (microCT) scanning, to detect and analysis various data indicators: Bone volume (BV), relative bone volume (BV/trabecular volume (TV)), cortical bone area (Ct.Ar), cortical bone thickness (Ct.Th), bone surface (BS), ratio of bone surface area to bone volume (BS/TV), bone mineral content (BMC), bone mineral density (BMD), trabecular number (Tb.N), trabecular separation/Spacing(Tb.Sp), and trabecular thickness (Tb.Th). After microCT (SCANCO, Wangen-Brüttisellen, Switzerland) scanning, mouse tibias were fixed with 4% paraformaldehyde and decalcified with 10% EDTA for 4 weeks, and paraffin-embedded sectioning was performed. After hematoxylin and eosin (HE) staining, the sections were observed and analyzed under a microscope.

MicroRNA Sequencing Analysis

When the P3 generation HucMSCs grew to 80% confluence, they were divided into three groups, and each group had three samples. The control group was replaced with conditioned medium without exosome serum, and the supernatant was collected after 48 h of culture; osteogenic group 3 and osteogenic group 7 were replaced with osteogenic induction differentiation medium containing 10% exosome-free serum, and the supernatant was collected after 48 h and 7 days of culture, respectively. The cell supernatants of the three groups were separated by ultracentrifugation. RNA sequencing uses next generation sequencing (NGS) technology was used to obtain the sequences of miRNAs (18–30 nt or 18–40 nucleotides) in

exosomes. Sequencing data were then compared with databases to identify and analyze the small RNA sequences.

The sequencing results of three groups of miRNAs analyzed statistically for differentially expressed miRNAs. The *p*-value was corrected by multiple hypothesis tests using the Q value. Genes with two or more coincidence differences and a Q-value less than or equal to 0.001 were considered as significant differentially expressed genes. The domain value of *p*-value was determined by controlling the FDR (False Discovery Rate). The FDR value of the difference test was obtained, and the multiple of differential expression of a gene between different samples was calculated according to the expression amount of the gene, as calculated using the FPKM value (Fragments Per Kilobase of transcript per Million mapped reads). The smaller the FDR value, the greater the difference multiples, indicating more significant expression differences. Differentially expressed genes were defined as those with an FDR < 0.001 and > 2-fold expression difference.

RNAhybrid [13], miRanda [14], and TargetScan [15] were used to predict the potential target genes of the miRNAs, and then the intersections of the results predicted by three software were noted. According to the results of differential miRNA detection, hierarchical clustering analysis was performed using the pheatmap function in the R software to form a clustering heat map of differentially expressed miRNAs between the groups. The biological functions of genes were investigated using Kyoto Encyclopedia of Genes and Genome (KEGG) Pathway analysis. According to KEGG Pathway [16] public database, pathway significance enrichment analysis was carried out to identify those pathways that were significantly enriched in candidate genes compared with the whole genome background. Pathways with a Q value < 0.05 were defined as pathways that were significantly enriched in differentially expressed genes. Pathway significant enrichment can identify the most important biochemical metabolic pathways and signal transduction pathways in which the candidate genes participate.

Statistical analysis

Statistical analysis was performed using the software Statistical Product and Service Solutions (SPSS)19.0 (IBM Corp., Armonk, NY, USA). GraphPad Prism 8.0 (GraphPad. Inc, La Jolla, CA, USA) and ImageJ Launcher software (NIH, Bethesda, MD, USA) were used for image editing and gray value analysis, respectively. The two groups were compared and analyzed using *t*-tests. Differences were considered significant at $P < 0.05$ (*$P < 0.05$, **$P < 0.01$, ***$P < 0.001$, and ****$P < 0.0001$).

Results

Typical features of hucMSCs and hucMSC-derived exosomes

HucMSCs isolated from Wharton's Kelly's tissue of the umbilical cord are typically fusiform, triangular, or fibrous. When they approach maturity, they appear to from a whirlpool or broom shape. When HucMSCs differentiated into osteoblasts, Alizarin red could stain the mineralized nodules red or orange red; when they differentiated into adipocytes, oil red dye could dye the fat drops in adipocytes orange red; after 30

days of induction, chondrocytes were formalin-fixed and paraffin-embedded, and finally stained with alixin blue, which partly showed the endo-acidic mucopolysaccharides in cartilage tissue (see Figure 1A). Flow cytometry showed that the hucMSCs were positive for CD73, CD90, and CD105; and negative for CD45, CD34, CD11b, CD19, and HLA-DR (see Figure 1B). Electron microscopy showed that the exosomes were typical vesicles(see Figure 1C). The particle size range of exosomes suspension was 20–200 μm (see Figure 1D). Western blotting analysis indicated that the hucMSC-derived exomes contained exosomal markers such as CD9, CD81, and tumor susceptibility 101 (TSG101).(see Figure 1E)

Effect of exosomes on the proliferation and differentiation of osteoblasts

After co-culture of Exo1 with OB cells for 36 h and 60 h, the absorbance of OD450 was measured by CCK-8, and it was found that Exo1 significantly promoted OB proliferation in a concentration-dependent manner (see Figure 2A), but the concentration gradients of Exo2 were not significantly different from those of the control group (see Figure 2B).

When the concentration of exosomes was 100 μg/ml, staining for OB differentiation was deepest in the Exo2 group, which indicated that Exo2 could promote osteogenesis better than Exo1 (see Figure 2C-D). Compared with the control group, the cells in the Exo1 and Exo2 groups were stained deeply, and there were many mineralized deposits. When the concentration of exosomes was adjusted to 200 μg/ml, the staining depth and mineralized deposits increased with the increase in concentration (see Figure 2E-H), which showed that exosomes could promote osteogenic differentiation in a concentration dependent manner. After coculture of exosomes and osteoblasts, western blotting showed that the levels of RUNX2, COL1A1, ALP, and OST in the cells of the Exo1 and Exo2 groups were higher than those of the control group, and the levels of RUNCX2, ALP and OST in Exo2 group showed the most significant increase (see Figure 3A-B).

The effect of exosomes on osteoporosis in an animal model

Six weeks after exosomes application, three-dimensional reconstruction images of tibia and cancellous bone were scanned using micro CT in OVX+Exo1 group, OVX+Exo2 group, OVX group, OVX+E2 group, and sham group (see Figure 4A). After statistical analysis of BV/TV, BMD, Conn.D, tb.n, tb.sp and SMI, it was confirmed that exogroup 1 and Exo2 had a certain therapeutic effect on osteoporosis compared with the OVX group (see figure 4B). Paraffin sections of mouse tibia and cancellous bone were stained with HE.Compared with the OVX group, the degree of osteoporosis was significantly reduced in the Exo1 and Exo2 groups (see Figure 3C).

Expression of microRNA in exosomes

As can be seen from the differential miRNA heat map (see Figure 5A-B), the changes of differentially expressed miRNAs in each group, and the number of differentially expressed miRNAs gradually increased with prolonged osteogenic differentiation.

The predicted target genes of the differentially expressed miRNAs were analyzed by KEGG Pathway enrichment (see Figure 6A-B). We found that target genes in the control vs. osteogenic 3 comparison were enriched in the osteoclast differentiation pathway and peroxisome proliferator activated receptor (PPAR) signaling pathway. The PPAR signaling pathway is important for MSC to differentiate into adipocytes. Therefore, the regulation by miRNAs of the PPAR signaling pathway might be one of the mechanisms by which exosomes regulate cell differentiation and treat osteoporosis.

Osteoclast differentiation, osteoblast differentiation, and the PPAR signaling pathway are closely related to the occurrence and development of osteoporosis. Three miRNAs related to the above signal pathways were screened out: Hsa-mir-328-3p, hsa-mir-2110, and hsa-let-7c-5p. The target genes related to the above signal pathways were screened miRNA target gene prediction. The target of hsa-mir-328-3p was *CHRD* (chordin). Hsa-mir-2110 was predicted the target TNF, and hsa-let-7c-5p was predicted to target PPARG (peroxisome proliferator activated receptor gamma). The expression these miRNA in each group and the base complementary pairing sequence of miRNA 3´-UTR region with target gene are shown in Figure 6C

Discussion

Exosomes are carriers and transfer agents of intercellular information, and the study of exosomes is important to reveal the mechanism of intercellular information exchange. As physiological vesicles, exosomes can be targeted to alter specific regulatory cell function materials they contain to improve the accuracy and effectiveness of treatment. The use of cell-derived vesicles can reduce the risks associated with transplantation and minimize the possible immune response and ectopic tissue development problems caused by MSC transplantation [1,9,17]. Experimental studies showed that exosomes derived from MSCs have therapeutic effects on many diseases, and their cargoes are important to regulate cell function and play a therapeutic role [17]. Therefore, the present study aimed to explore the mechanism of exosomes-related osteogenic differentiation, and identify targets related to the proliferation and differentiation of osteoblasts.

Previous studies have proved that the exosomes from HucMSCs have therapeutic effects in a variety of diseases, such as immune diseases, Alzheimer's disease, inflammatory bowel disease, spinal cord nerve injury, cancer, and ischemia, which are similar to the therapeutic effects of HucMSCs [5,18]. To further explore the effect of exosomes on osteogenic differentiation, we isolated the exosomes produced by HucMSCs. Preparations Exo1 and Exo2 could promote osteogenic differentiation, as observed using ALP and alizarin red staining; however, the effect of Exo2 was more obvious. Western blotting showed that the levels of osteogenic differentiation-related proteins RUNX2, COL1A1, ALP, and OST were higher in the two exosome preparation than that in the blank control group, and was concentration dependent.[19]. The results of CCK-8 showed that Exo1 could promote the proliferation of osteoblasts, while Exo2 did not. These results showed that in the microenvironment of osteogenic differentiation, the regulatory function of exosomes had changed, and the effect of exosomes on osteogenic differentiation was enhanced; the microenvironment reduced the promoting effect on OB proliferation.

Osteoporosis is caused by an imbalance of the differentiation ratio of MSCs to osteoblasts and adipocytes, decreased numbers of osteoblasts, enhanced osteoclast activity, and the increase in bone absorption caused by changes of the microenvironment, such as ageing and estrogen deficiency [19,20]. The differentiation direction of MSCs is affected by the microenvironment, and the expression and inhibition of various related genes in cells will also change markedly. Therefore, changes in exosome function in different microenvironments might play an important role in the regulation of osteoporosis.

According to the analysis of BV/TV, BMD, BS / BV, conn.d, TB. N, TB. SP, TB. Th, SMI, and the 3D reconstruction images, Exo1 and Exo2 appeared to have therapeutic effects on osteoporosis. Although Exo 2 strongly promoted osteogenic differentiation, there was no statistical difference between Exo 1 and Exo 2 data in the animal models. It is possible that some exosomes lose their activity when they enter the body. In addition, MSCs affected by the microenvironment of osteogenic differentiation gradually differentiate into osteoblasts, and the expression of proliferation information is reduced; therefore, the exosomes may lack material information to promote proliferation or regulate other functions. For example, studies have confirmed that HucMSC-derived exosomes have the functions of local regulation of osteogenic differentiation, promotion of cell proliferation, promotion of angiogenesis, and regulation of immune response [5,18].

The core mechanism of microRNAs is to induce mRNA degradation or inhibit the expression of their target genes through complementary pairing with mRNA base sequences, which is a key mechanism of biological processes such as cell differentiation, growth, migration, and apoptosis [7]. Exosomes are carriers of information between cells or tissues; therefore, microRNAs in exosomes play an important role in the regulation of cell function [21]. It can be seen from the differential miRNA thermogram that in an osteogenic differentiation environment, with the extension of time, the type and expression of miRNAs are constantly changing, indicating that changes in the microenvironment can affect the cargoes of exosomes. In the bubble diagram of KEGG pathway enrichment, some miRNA target genes were enriched in two metabolic pathways of Osteoclast differentiation and PPAR signaling pathway related to fat differentiation, which was consistent with the pathological changes observed in the process of osteoporosis [19,20].

In the prediction of microRNA targeting genes, it was found that *CHRD* was the target of hsa-mir-328-3p. Chordin binds to bone morphogenetic protein (BMP) and inhibits the activation of BMP related signaling pathways [29]. The results suggested that the inhibition of *CHRD* expression led to the significant increase in ALP expression and extracellular mineral deposition. Chordin might represent a new target to promote bone regeneration [22,23]. The target gene of hsa-mir-2110 was *TNF* (tumor necrosis factor). The TNF superfamily is mainly secreted by macrophages. It can bind to and act through its receptors TNFRSF1A/TNFR1 and TNFRSF1B/TNFBR. TNFs are involved in a wide range of biological processes, including cell proliferation, differentiation, apoptosis, lipid metabolism, and coagulation. In the process of osteoclast differentiation, TNF plays an important role in the differentiation and formation of osteoclasts. It is a necessary inducting factor of almost all osteoclast differentiation signaling pathways [20]. Hsa-let-7c-5p was predicted to target *PPARG.* PPARgamma is a member of the PPAR subfamily. There are three

types of PPAR: PPARalpha, PPARdelta, and PPARgamma. Among them, PPARgamma is the key regulator of adipocyte differentiation. In addition, PPARgamma is involved in the pathology of many diseases, including obesity, diabetes, atherosclerosis, and cancer [7]. A study of bone marrow MSCs in the elderly with osteoporosis showed that the osteogenic differentiation ability of MSCs decreases, their ability to differentiate into adipocytes increases, and the osteoclast activity increases. Therefore, hsa-mir-2110 and hsa-let-7c-5p could be developed as targets to alleviate osteoporosis [24].

The expression levels of hsa-mir-328-3p and hsa-mir-2110 were significantly higher in the experimental groups of osteogenic 3 and 7 than in the controls. Moreover, hsa-mir-2110 targets members of osteoclast differentiation related signaling pathways. Hsa-let-7c-5p showed no significant difference in expression between osteogenic 3 and the control, but increased significantly in experimental group of osteogenic 7. Therefore, microRNAs in exosomes might target genes to inhibit adipose differentiation and osteoclast activity in the early stage of osteogenic differentiation.

Conclusions

In the microenvironment of osteoblast differentiation culture, hucMSC-derived exosomes can significantly promote the differentiation of osteoblasts, and displayed certain therapeutic and preventative effects on an OVX mouse osteoporosis model. It is suggested that exosomes are influenced by the cells in the differentiation stage and carry related substances to promote osteoblast differentiation. Bioinformatic analysis showed that osteogenic differentiation changed the microRNA profile in exosomes, and the target genes of these miRNAs might not only act on osteogenic differentiation, but also on the pathways related to adipogenic differentiation and osteoclastic differentiation of MSCs. Therefore, the prevention and treatment of osteoporosis may be subjected to multifaceted regulation.

Abbreviations

MSC: Mesenchymal stem cell, HucMSC: Human umbilical cord MSCs, Exo1: Exosomes from standardized stem cell culture, Exo2: osteogenic differentiation-exosomes, OB: Osteoblast, RUNX2: RUNX family transcription factor 2, OST: osteopontin, COL1A1: collagen type I alpha 1 Chain, ALP: Alkaline phosphatase, OVX: ovariectomized, E2: Estradiol, BV/TV: Bone volume to total tissue volume ratio, Ct.Ar: cortical bone area, Ct.Th: cortical bone thickness, BS/TV: ratio of bone surface area to bone volume, BMD: bone mineral density, Tb.N: trabecular number, Tb.Sp: trabecular separation/Spacing, Tb.Th: trabecular thickness, Conn.D: Connective density; SMI: Structure Model Index.

Declarations

Acknowledgements

We thank the Central Laboratory of Medical College of Shantou University for its aid and technical support.

Funding

This work was supported by the Guangdong Science and Technology Special Fund Mayor Project (No: 20190301-65), 2020 Li Ka Shing Foundation Cross-Disciplinary Research Grant (2020LKSFG01D) and Shantou City Science and Technology Plan Project, Guangdong Province, China (No: 2018155, 2019-106-37). The funding bodies had no role in the design of the study and the collection, analysis, and interpretation of the data and the writing the manuscript. The corresponding author had full access to all the data in the study and had final responsibility for the decision to submit for publication.

Availability of data and materials

All data generated or analyzed during this study are included in this article.

Authors' contributions

Ge Yahao performed the experiments and created the graphs and wrote the manuscript. Wang Xinjia contributed to the conception and design, financial and administrative support, and manuscript reviewing and revising.

Ethics approval

This experimental study was approved by the Medical Laboratory Animal Ethics Committee, and all experimental procedures were in accordance with the procedures of the Medical Laboratory Animal Center of Shantou University Medical College.

Consent for publication

Not applicable.

Conflicts of Interest

The authors declare that they have no competing interests.

References

1. Phinney DG, Pittenger MF: Concise Review: MSC-Derived Exosomes for Cell-Free Therapy. Stem Cells. 2017; 354:851-858.

2. Phan J, Kumar P, Hao D, Gao K, Farmer D, Wang A: Engineering mesenchymal stem cells to improve their exosome efficacy and yield for cell-free therapy. J Extracell Vesicles. 2018; 71:1522236.

3. Gimona M, Pachler K, Laner-Plamberger S, Schallmoser K, Rohde E: Manufacturing of Human Extracellular Vesicle-Based Therapeutics for Clinical Use. Int J Mol Sci. 2017; 186.

4. Lai RC, Yeo RW, Lim SK: Mesenchymal stem cell exosomes. Semin Cell Dev Biol. 2015; 40:82-88.

5. Yaghoubi Y, Movassaghpour A, Zamani M, Talebi M, Mehdizadeh A, Yousefi M: Human umbilical cord mesenchymal stem cells derived-exosomes in diseases treatment. Life Sci. 2019; 233:116733.

6. Mendt M, Rezvani K, Shpall E: Mesenchymal stem cell-derived exosomes for clinical use. Bone Marrow Transplant. 2019; 54Suppl 2:789-792.

7. Seenprachawong K, Tawornsawutruk T, Nantasenamat C, Nuchnoi P, Hongeng S, Supokawej A: miR-130a and miR-27b Enhance Osteogenesis in Human Bone Marrow Mesenchymal Stem Cells via Specific Down-Regulation of Peroxisome Proliferator-Activated Receptor gamma. Front Genet. 2018; 9:543.

8. Kwong FN, Richardson SM, Evans CH: Chordin knockdown enhances the osteogenic differentiation of human mesenchymal stem cells. Arthritis Res Ther. 2008; 103:R65.

9. Zhang J, Liu X, Li H, Chen C, Hu B, Niu X *et al*: Exosomes/tricalcium phosphate combination scaffolds can enhance bone regeneration by activating the PI3K/Akt signaling pathway. Stem Cell Res Ther. 2016; 71:136.

10. Ma Z, Cui X, Lu L, Chen G, Yang Y, Hu Y *et al*: Exosomes from glioma cells induce a tumor-like phenotype in mesenchymal stem cells by activating glycolysis. Stem Cell Res Ther. 2019; 101:60.

11. Naji A, Eitoku M, Favier B, Deschaseaux F, Rouas-Freiss N, Suganuma N: Biological functions of mesenchymal stem cells and clinical implications. Cell Mol Life Sci. 2019; 7617:3323-3348.

12. Lian Z, Han J, Huang L, Wei C, Fan Y, Xu J *et al*: Retraction of: A005, a novel inhibitor of phosphatidylinositol 3-kinase/mammalian target of rapamycin, prevents osteosarcoma-induced osteolysis. Carcinogenesis. 2019; 402:e1-e13.

13. Kruger J, Rehmsmeier M: RNAhybrid: microRNA target prediction easy, fast and flexible. Nucleic Acids Res. 2006; 34Web Server issue:W451-454.

14. John B, Enright AJ, Aravin A, Tuschl T, Sander C, Marks DS: Human MicroRNA targets. PLoS Biol. 2004; 211:e363.

15. Agarwal V, Bell GW, Nam JW, Bartel DP: Predicting effective microRNA target sites in mammalian mRNAs. Elife. 2015; 4.

16. Kanehisa M, Araki M, Goto S, Hattori M, Hirakawa M, Itoh M *et al*: KEGG for linking genomes to life and the environment. Nucleic Acids Res. 2008; 36Database issue:D480-484.

17. Elahi FM, Farwell DG, Nolta JA, Anderson JD: Preclinical translation of exosomes derived from mesenchymal stem/stromal cells. Stem Cells. 2020; 381:15-21.

18. Yin S, Ji C, Wu P, Jin C, Qian H: Human umbilical cord mesenchymal stem cells and exosomes: bioactive ways of tissue injury repair. Am J Transl Res. 2019; 113:1230-1240.

19. Chen Q, Shou P, Zheng C, Jiang M, Cao G, Yang Q *et al*: Fate decision of mesenchymal stem cells: adipocytes or osteoblasts? Cell Death Differ. 2016; 237:1128-1139.

20. Park-Min KH: Metabolic reprogramming in osteoclasts. Semin Immunopathol. 2019; 415:565-572.

21 Kusuma GD, Carthew J, Lim R, Frith JE: Effect of the Microenvironment on Mesenchymal Stem Cell Paracrine Signaling: Opportunities to Engineer the Therapeutic Effect. Stem Cells Dev. 2017; 269:617-631.

22. Troilo H, Barrett AL, Wohl AP, Jowitt TA, Collins RF, Bayley CP, Zuk AV, Sengle G, Baldock C: The role of chordin fragments generated by partial tolloid cleavage in regulating BMP activity. Biochem Soc Trans. 2015; 435:795-800.

23. Vizoso FJ, Eiro N, Cid S, Schneider J, Perez-Fernandez R: Mesenchymal Stem Cell Secretome: Toward Cell-Free Therapeutic Strategies in Regenerative Medicine. Int J Mol Sci. 2017; 189.

24. Valenti MT, Dalle Carbonare L, Mottes M: Osteogenic Differentiation in Healthy and Pathological Conditions. Int J Mol Sci. 2016; 181.

Figures

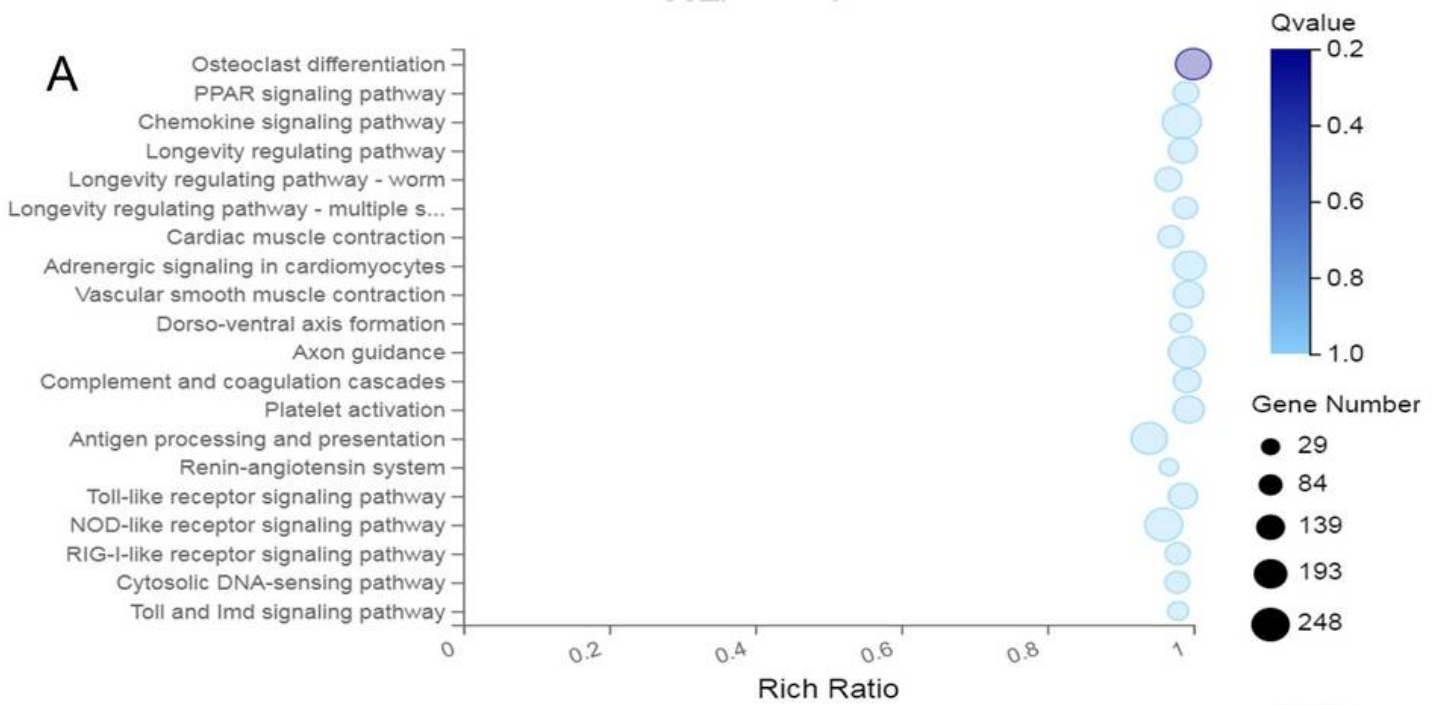

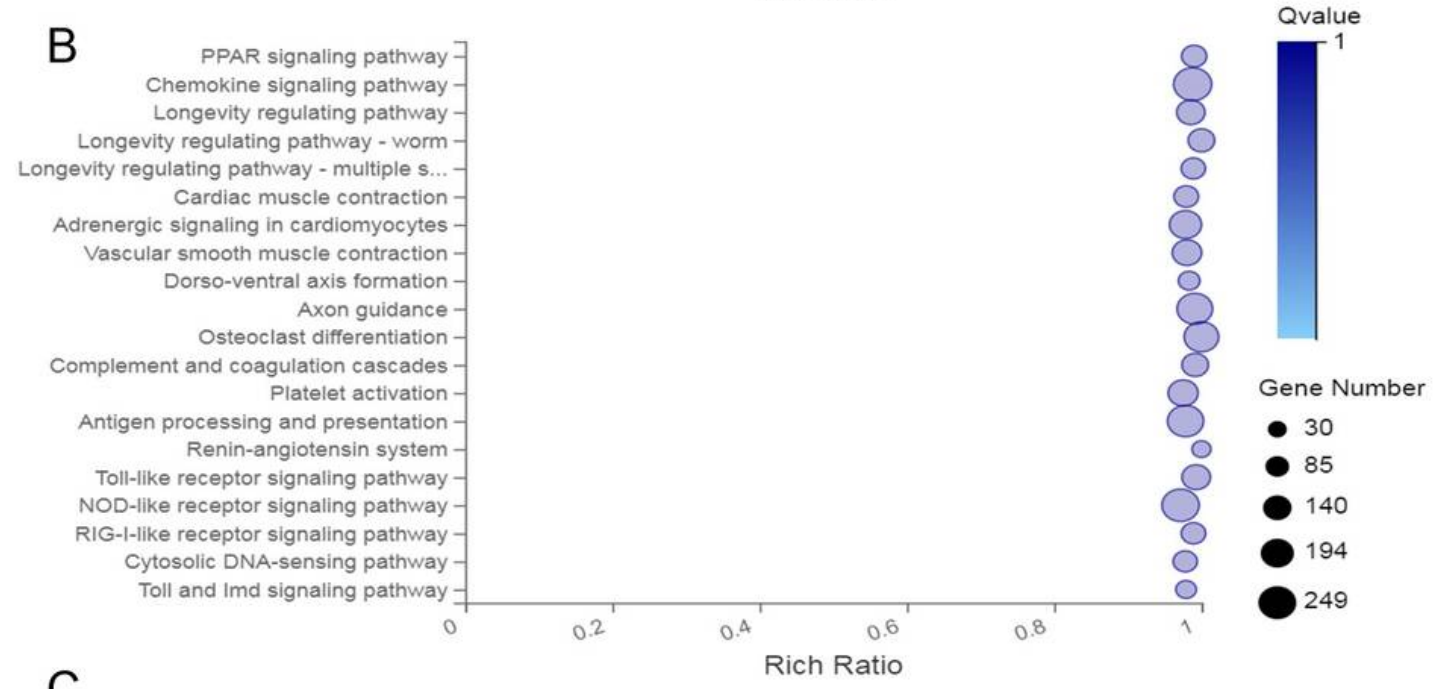

C

Gene ID	Compare Group	log2Ratio	Qvalue
hsa-miR-328-3p	control-vs-osteogenic3	1.867586949	0
hsa-miR-328-3p	control-vs-osteogenic7	2.19413482	0
hsa-miR-328-3p	osteogenic3-vs-osteogenic7	0.326547872	4.60E-53
hsa-miR-2110	control-vs-osteogenic3	1.087768336	1.10545E-32
hsa-miR-2110	control-vs-osteogenic7	1.348170145	7.06311E-85
hsa-miR-2110	osteogenic3-vs-osteogenic7	0.260401809	2.81018E-05

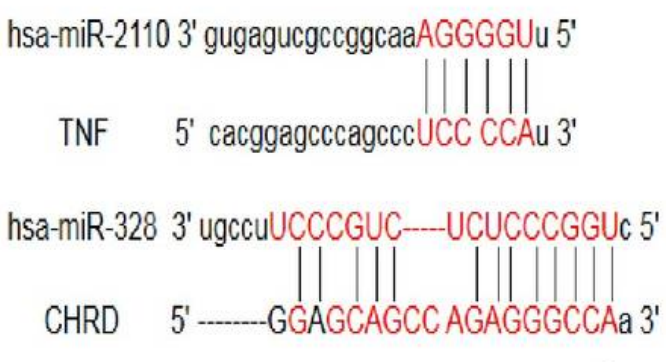

Figure 1

MiRNA target enrichment and KEGG analysis for HucMSC exosomes. A. Control vs. osteogenic 3 differentially expressed miRNA target gene enrichment bubble map. B. Control vs. osteogenic 7 differentially expressed miRNA target gene enrichment bubble map. The X-axis is the enrichment ratio (the ratio of the number of genes annotated to an item in a selected gene set to the total number of genes annotated to that item by the species), and the Y-axis is KEGG Pathway; the size of the bubble represents the number of genes annotated to a KEGG Pathway. The color represents the enrichment Q value, and a darker color represents a smaller the Q value. Compared with control group, osteogenic 3 and osteogenic 7 were significantly enriched in Osteoclast differentiation and PPAR signaling pathways in the KEGG Pathway analysis, indicating that exosome function is closely related to osteoclast differentiation and adipose differentiation. The bubble map in B indicated that the target genes enriched in Osteoclast differentiation and PPAR signaling pathway increased greatly in the osteogenic group7. C. The left is the differential analysis of hsa-mir-328-3p and hsa-mir-2110 in each group, and the right is the base complementary pairing sequence of the miRNA 3´-UTR region with the target gene.

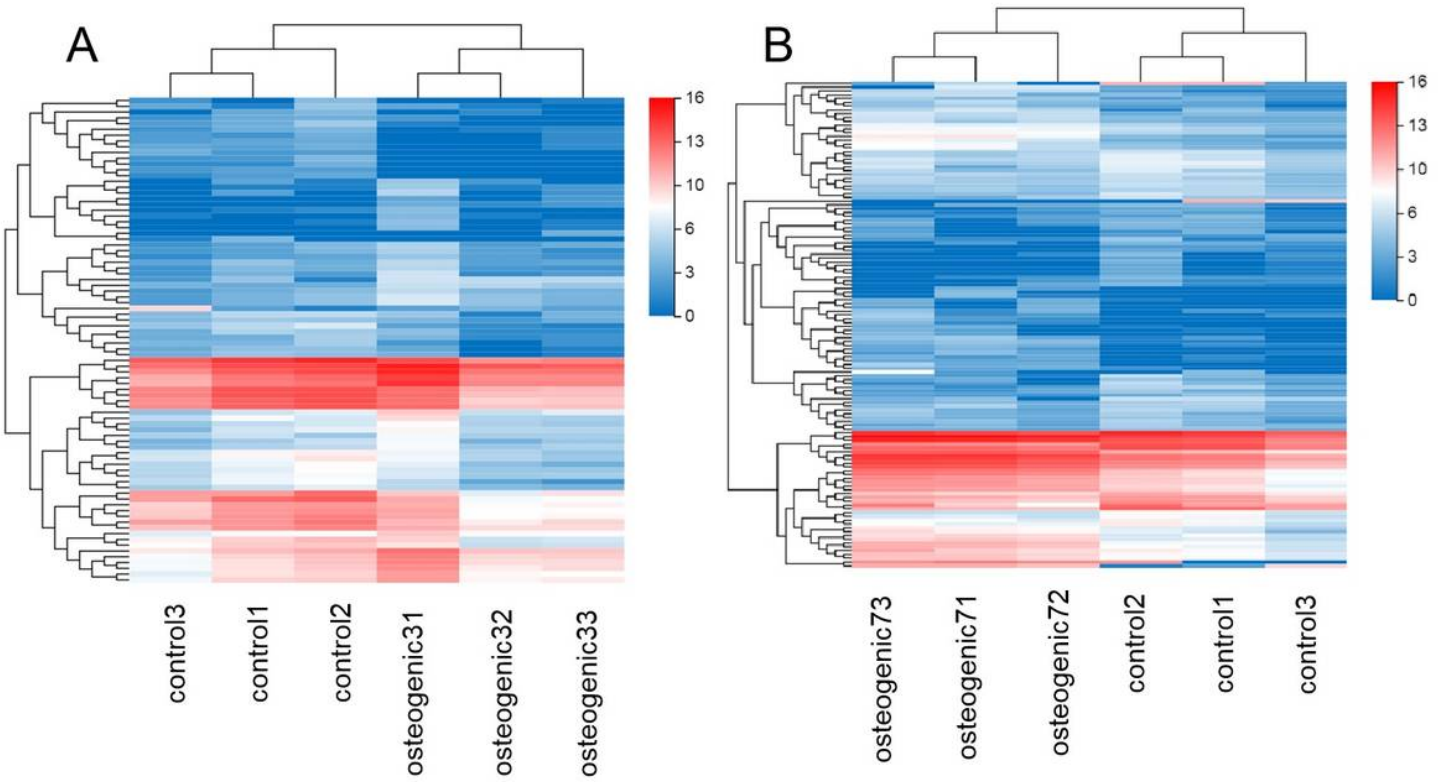

Figure 2

The osteogenic microenvironment affects the miRNA profile of HucMSC exosomes. A. Control vs. osteogenic 3 differentially expressed genes miRNA clustering heat map. B. Control vs. osteogenic 7 differentially expressed genes miRNA clustering heatmap, showing the expression level of differentially expressed genes by color, with log2 (expression value + 1) of the sample on the horizontal axis and genes on the vertical axis. The redder the color of the block, the higher the expression level; the bluer the color, the lower the expression level. Compared with the control group, the changes of the differentially expressed genes of the miRNAs in the osteogenic 3 group were obvious, indicating that the changes of the exosomal miRNAs were affected by the microenvironment of osteogenic differentiation. Compared with the control group, the number of differentially expressed genes in the Osteogenic 7 group increased, and the expression changes were more obvious, indicating that with the prolongation of induction differentiation time, the microenvironment had a greater impact on exosomes.

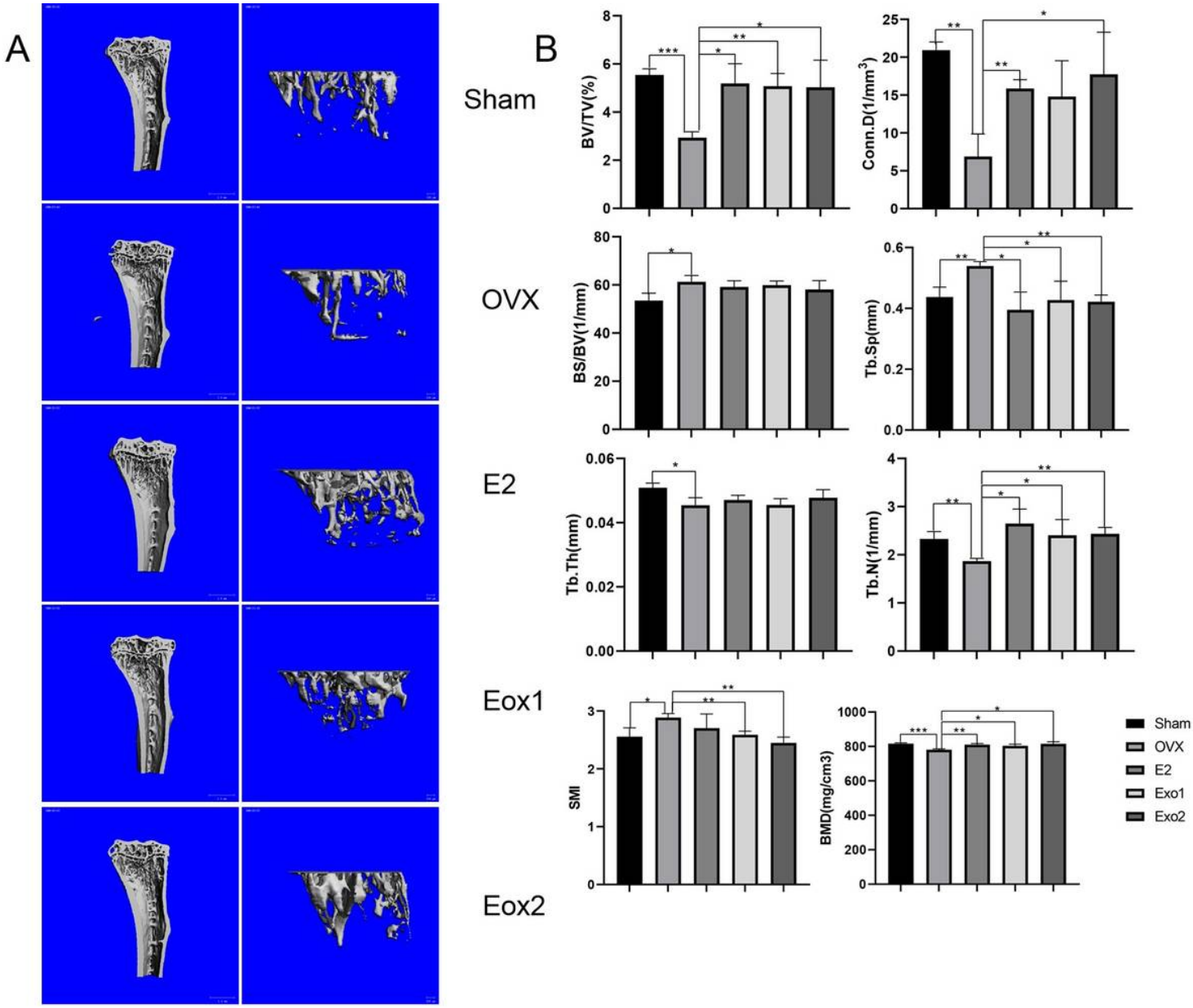

Figure 3

Therapeutics effects of HucMSC exosomes in osteoporosis model mice. A. MicroCT scans of tibia and cancellous bone of mice after 6 weeks, showing that Exo1 and Exo2 induced increased bone mass relative to the Sham group in three-dimensional images. B. Compared with the control group, after statistical analysis, the relative bone volume (BV/TV), bone density (BMD), trabecular Connectivity density (Conn.D), trabecular number (Tb.N), trabecular separation (Tb.Sp), and trabecular structure pattern index (SMI) were significantly different, and the results demonstrated that Exo1 and Exo2 had therapeutic effects on osteoporosis.

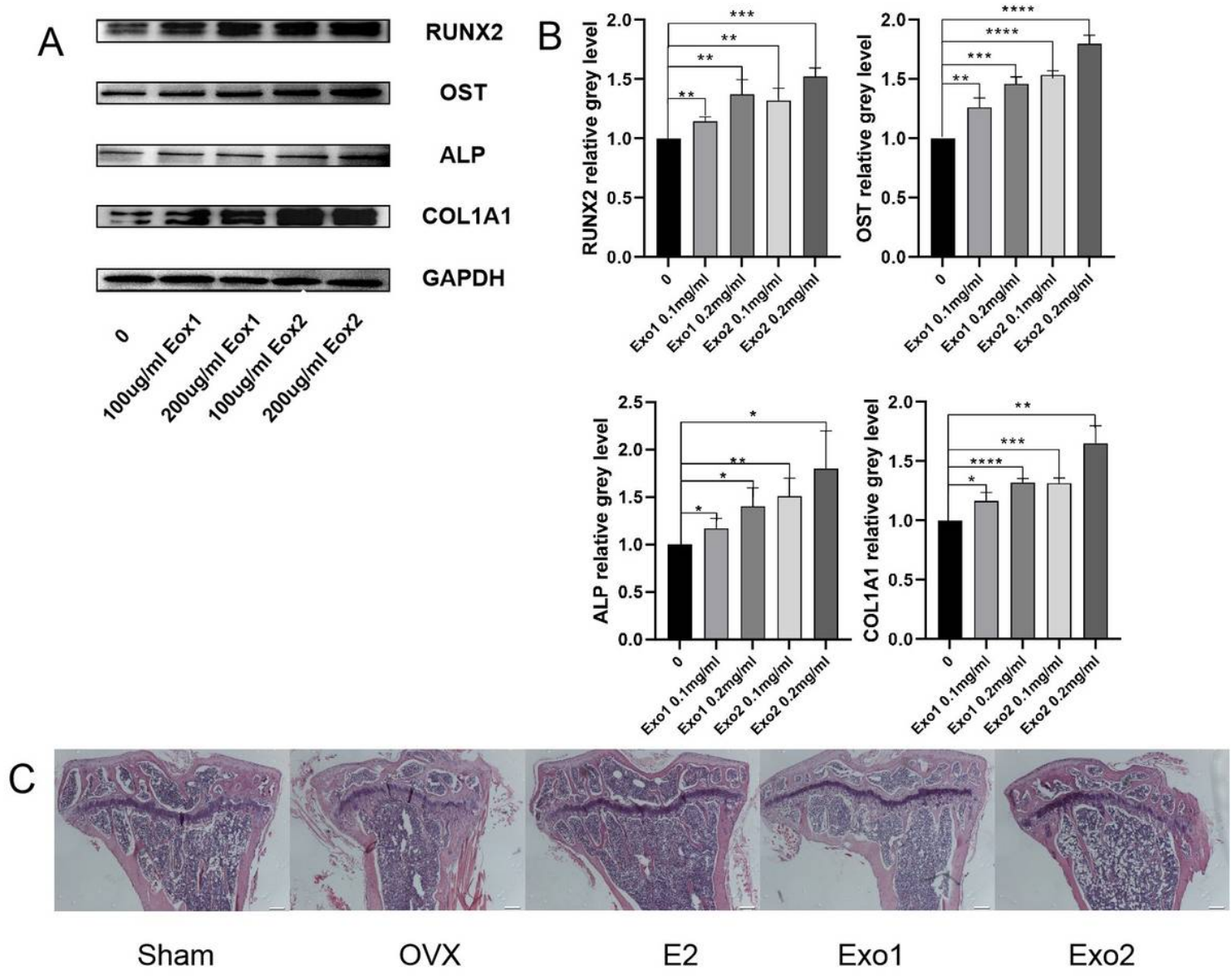

Figure 4

HucMSC exosomes promote osteoblast differentiation, affect osteoblast differentiation-related protein levels, and reduce osteoporosis. A. Western blotting validation of the effects of Exo1 and Exo2 on the levels of RUNX2, COL1A1, ALP, and OST proteins in OB cells. The exosomes promoted the differentiation of osteoblasts in a concentration-dependent manner, and Exo2 showed a stronger effect on promoting osteogenic differentiation than Exo1. B. Statistical analysis of the expression of osteoblast differentiation-related proteins showed that the levels of RUNX2, COL1A1, ALP, and OST in the Exo1 group and Exo2 group were significantly higher than that in the control group. C. HE staining of bone tissue sections of mice, compared with OVX group, showed that osteoporosis was reduced in the Exo1 group and Exo2 group (shown at original magnification, × 50).

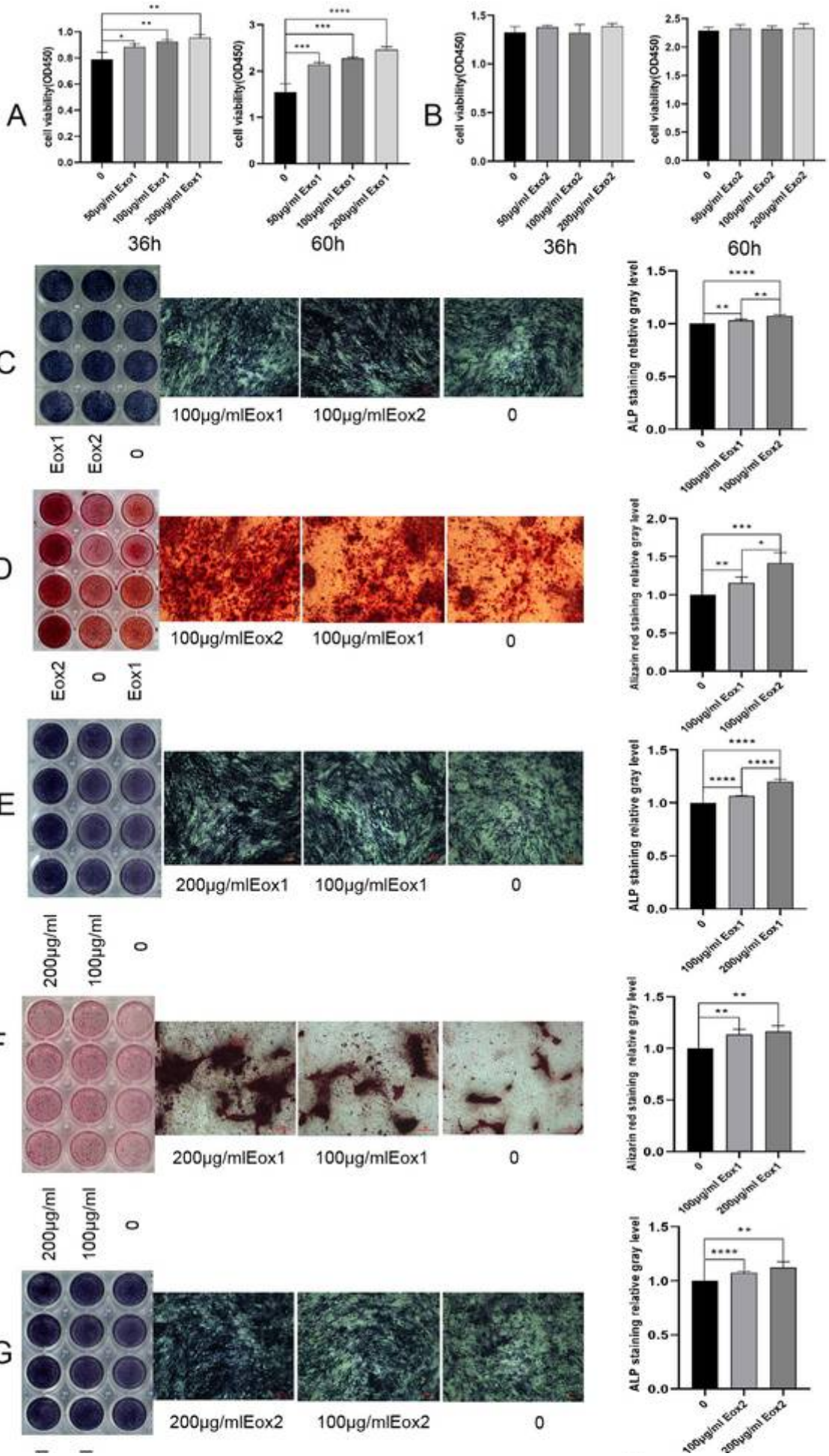
A
cell viability(OD450)
0
50μg/ml Exo1
100μg/ml Exo1
200μg/ml Exo1
36h
60h
B
cell viability(OD450)
0
50μg/ml Exo2
100μg/ml Exo2
200μg/ml Exo2
36h
60h
C
100μg/mlEox1
100μg/mlEox2
0
Eox1
Eox2
0
ALP staining relative gray level
D
100μg/mlEox2
100μg/mlEox1
0
Eox2
0
Eox1
Alizarin red staining relative gray level
E
200μg/mlEox1
100μg/mlEox1
0
200μg/ml
100μg/ml
0
ALP staining relative gray level
F
200μg/mlEox1
100μg/mlEox1
0
200μg/ml
100μg/ml
0
Alizarin red staining relative gray level
G
200μg/mlEox2
100μg/mlEox2
0
ALP staining relative gray level

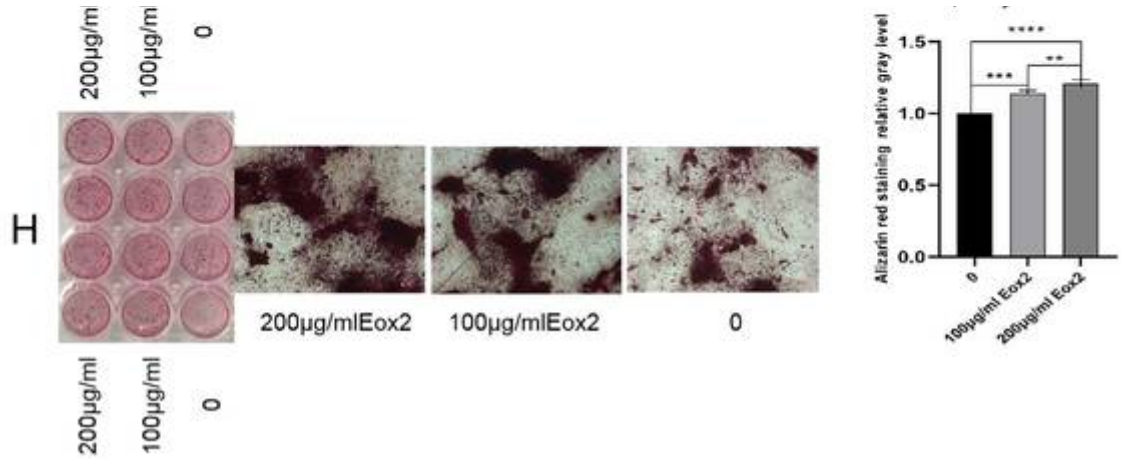

Figure 5

HucMSC exosomes promote osteogenic proliferation and differentiation. A. After co-culture of Exo1 with OB cells, the results of CCK-8 assays showed a significant promoting of proliferation in a concentration-dependent manner. B. Exo2 did not promote proliferation after co-culture with OB cells. Exo1 and Exo2 concentrations were 100 □g/ml. C. Images show ALP staining, in which the color in the Exo2 image was darker than that for Exo1. D. Images show alizarin red staining, in which Exo2 produced the most mineralized nodules, indicating that Exo2 promotes stronger osteogenic differentiation than Exo1. The concentration of Exo1 was set at 200, 100, and 0 □g/ml, and the concentration of Exo2 was set at 200, 100, and 0□g/ml. E and G show ALP staining, and F and H Alizarin red staining of exosomes. The staining increased with increasing concentration, indicating that Exo1 and Exo2 promoted osteogenic differentiation in a concentration-dependent manner (shown at the original magnification, × 100).

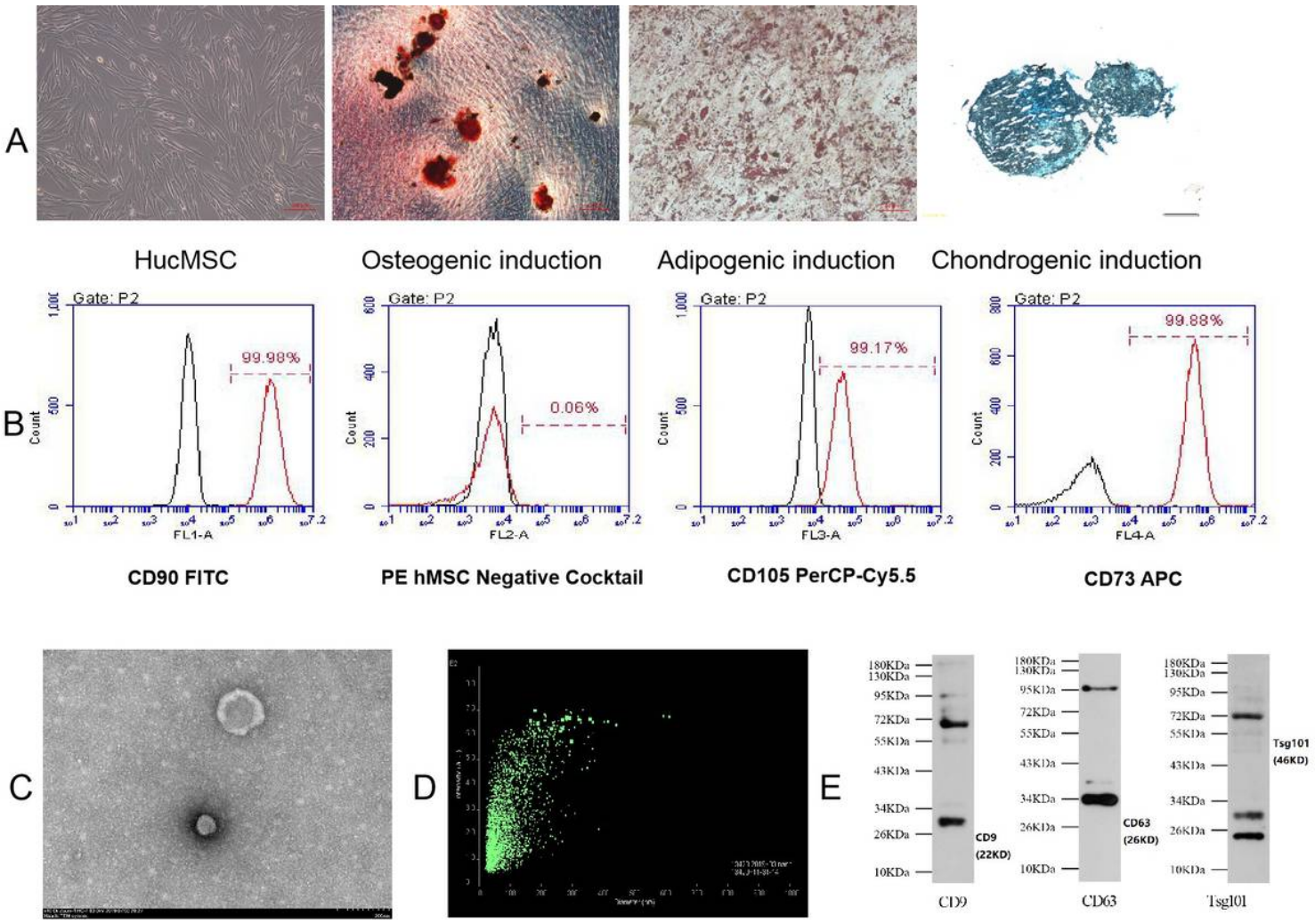

Figure 6

Structure and appearance of HucMSCs and their exosomes. A. HucMSCs have a whirlpool-like or broom-like appearance. Mineralized nodules induced by HucMSC osteogenic differentiation are stained red by Alizarin red (shown at original magnification, × 100). Fat droplets induced by HucMSC adipose differentiation are stained orange with oil red stain(shown at original magnification, × 200). Endoacid mucopolysaccharides formed by HucMSC cartilage differentiation were stained blue by alixin blue(shown at original magnification, × 100). B. Flow cytometry detected positive expression of HucMSC CD73, CD90, and CD105, and negative expression of CD45, CD34, CD11b, CD19, and HLA-DR. Black histograms represent the isotype controls, and the red peak represents the marker indicated. C. Under the electron microscope, the exosomes showed a double-layer membrane vesicle structure. D. The vesicle diameter in the sample suspension was distributed in the range of 20–200 □m. E. Western blotting confirmed that Exosome expressed CD9, CD63, TSG101 proteins.